group in addition to the interaction between the C=O and C—C bond orbitals.

Calculations. The geometry optimizations were carried out with the program GAMESS,[26] and the MP2-MP3 calculations were carried out with GAUSSIAN-82.[27]

(26) Dupuis, M.; Spangler, D.; Wendoloski, J. J. National Resource for Computation in Chemistry Program QG01, 1980.

(27) Binkley, J. S.; Frish, M. J.; De Frees, D. J.; Raghavachari, K.; Whiteside, R. A.; Schlegel, H. B.; Fluder, E. M.; Pople, J. A. Department of Chemistry, Carnegie-Mellon University, 1980.

MNDO Calculations of Ions in Chloroaluminate Molten Salts

Larry P. Davis,[†] **Chester J. Dymek, Jr.,**[*†] **James J. P. Stewart,**[†] **Henry P. Clark,**[‡] **and Walter J. Lauderdale**[‡]

Contribution from The Frank J. Seiler Research Laboratory, United States Air Force Academy, Colorado Springs, Colorado 80840-6528, and the Department of Chemistry, United States Air Force Academy, Colorado Springs, Colorado 80840-5791. Received December 26, 1984

Abstract: We have performed MNDO calculations on the anions in molten chloroaluminate salts. Calculated geometries for $AlCl_4^-$ and $Al_2Cl_7^-$ agree in most respects with available data. The vibrational spectrum of $Al_2Cl_7^-$ calculated by MNDO is consistent with the observed IR spectrum and leads to assignment of C_2 symmetry for this ion. The ^{27}Al NMR exchange reaction between the two anions was also studied. The calculated energy of activation in the most realistic model used was 13 kcal mol^{-1} compared to the experimental value of 10 kcal mol^{-1}.

Mixtures of 1-methyl-3-ethylimidazolium chloride (MEICl) and $AlCl_3$ are molten salts at and well below room temperatures.[1] The reaction forming this ionic liquid from the two substituents, which are solids at room temperature, is analogous to the reaction forming relatively low-melting inorganic chloroaluminate salts, such as $NaAlCl_4$, from NaCl and $AlCl_3$:

(1)
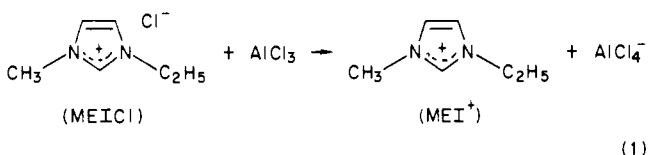
When $AlCl_3$ is added in less than stoichiometric amounts (i.e., the apparent mole fraction of $AlCl_3$, N, in the melts is less than 0.5), the anions in the melt are $AlCl_4^-$ and the excess Cl$^-$. Such melts are basic because Cl$^-$ acts as a Lewis base in the melts. When $N > 0.5$, the process

$$AlCl_3 + AlCl_4^- \rightarrow Al_2Cl_7^- \qquad (2)$$
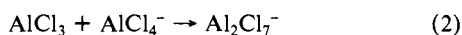
occurs, and the anions present are $AlCl_4^-$ and $Al_2Cl_7^-$. Since $Al_2Cl_7^-$ acts as a Lewis acid in the melts, such melts are acidic. Plots of the anion fractions of the anions as a function of N over the range $0 < N < 0.67$ are shown in Figure 1. These dependencies are calculated by using the well-justified assumption that the equilibrium constants for eq 1 and 2 are very large.[2] Further support of this assumption comes from the fact that large equilibrium constants have been deduced from the Raman spectra of similar room-temperature melts of 1-butylpyridinium chloride and $AlCl_3$.[3]

MEICl/$AlCl_3$ melts with compositions in the range $0.30 < N < 0.70$ are liquid below room temperature.[1] Properties of these melts, such as density, viscosity, and conductivity, have been reported for the range $0.30 < N < 0.70$.[4,5] Analysis of the dependence of these properties on N indicates that the coordination number of the MEI$^+$ in the melts is 2. NMR spectroscopy of the

melts[5] also supports the model in which each MEI$^+$ is closely associated with two anions, one above and one below the plane of its ring. Thus the overall structure may best be described as a collection of stacks of varying numbers of MEI$^+$–anion pairs, a model which would also explain the almost polymeric properties of the melts at lower temperatures.[5] Further support for this model comes from the results of Monte Carlo calculations in which the MEI$^+$ was represented by an oblate spheroid or plate and the anions were taken to be spherical.[6] These calculations predicted that the plates would tend to stack up with their planes parallel and with the spherical anions alternating between them. Thus in the range $0.50 < N < 0.67$, the MEI$^+$ ions are probably associated with $AlCl_4^-$ and $Al_2Cl_7^-$ ions as shown in Figure 2. Each stack shown is expected to extend indefinitely as suggested by the dotted lines.

NMR spectroscopy[7] has also been used to study the exchange reaction occurring in acidic melts between $Al_2Cl_7^-$ and $AlCl_4^-$:

$$Al^*Cl_4^- + Al_2Cl_7^- \rightarrow Al^*AlCl_7^- + AlCl_4 \qquad (3)$$

This reaction can be pictured as occurring between $AlCl_4^-$ and $Al_2Cl_7^-$ ions in adjacent stacks, as suggested by the double arrows in Figure 2. Reaction 3 has been observed in the ^{27}Al NMR peaks of the Al* in the $AlCl_4^-$ and $Al_2Cl_7^-$ environments in $N = 0.60$ melts, in which the two anions are in equal concentration. Use of the Bloch equation to simulate the ^{27}Al NMR line shapes at

(1) Wilkes, J. S.; Levisky, J. A.; Wilson, R. A.; Hussey, C. L. *Inorg. Chem.* **1982**, *21*, 1263.
(2) Dymek, C. J., Jr.; Williams, J. L.; Groeger, D. J.; Auborn, J. J. *J. Electrochem. Soc.* **1984**, *131*, 2887.
(3) Gale, R. J.; Gilbert, B.; Osteryoung, R. A. *Inorg. Chem.* **1978**, *17*, 2728.
(4) Fannin, A. A., Jr.; King, L. A.; Levisky, J. A.; Wilkes, J. S. *J. Phys. Chem.* **1984**, *88*, 2609.
(5) Fannin, A. A., Jr.; Floreani, D. A.; King, L. A.; Landers, J. S.; Piersma, B. J.; Stech, D. J.; Vaughn, R. L.; Wilkes, J. S.; Williams, J. L. *J. Phys. Chem.* **1984**, *88*, 2614.
(6) Murphy, R. D. Final Report—1984, USAF-SCEEE Summer Faculty Research Program, Frank J. Seiler Research Laboratory, U.S. Air Force Academy, CO 80840, 1984.
(7) Wilkes, J. S.; Frye, J. S.; Reynolds, G. F. *Inorg. Chem.* **1983**, *22*, 3870.

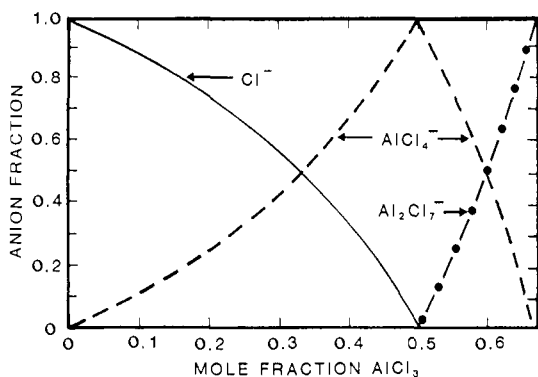†The Frank J. Seiler Research Laboratory.
‡Department of Chemistry.

5042 *J. Am. Chem. Soc., Vol. 107, No. 18, 1985*

Davis et al.

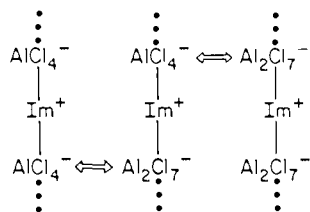**Figure 1.** Anion fractions in MEICl–AlCl₃ melts as a function of mole fraction of AlCl₃.

Figure 2. Model of associations of MEI⁺ with anions in acidic melts and sites for the ²⁷Al NMR exchange reactions.

various temperatures resulted in estimates of the rate constants for the two-site exchange reaction. An Arrhenius plot of the rate constant vs. temperature data gives a value for the energy of activation for the two-site exchange reaction of about 10 kcal/mol. Wilkes et al.[7] caution against using their data to calculate an exact value for the energy of activation for this NMR exchange process. In the absence of other data on this reaction, the value obtained from their data is the best estimate available.

In this paper, we report the results of semiempirical molecular orbital calculations on the chloroaluminate species in these melts. The focal point for this effort was to determine if the calculations were good enough to give a value for the energy of activation for the NMR exchange reaction, eq 3, close to the observed value of 10 kcal/mol. In the course of the calculations, we also compared the structures and force constants obtained for the $AlCl_4^-$ and $Al_2Cl_7^-$ species with spectroscopic results.[3,8-11] An interesting problem in this regard concerns the structure of $Al_2Cl_7^-$, in which two essentially tetrahedral $AlCl_4^-$ groups share a common Cl. This bridging Cl is bonded to the two Al's with the bond angle expected to be much less than 180° based on a conventional model in which the lone pairs on the Cl repel the two Al–Cl bonding orbitals. However, Raman and infrared spectra on molten inorganic chloroaluminate salts suggest that the Al–Cl–Al bond angle is 180°, corresponding to D_{3d} symmetry.[8-10] On the other hand, X-ray diffraction spectroscopy of $Al_2Cl_7^-$ in $Te_4^{2+}(Al_2Cl_7^-)_2$ yielded a nonlinear bridging angle.[11] Thus another goal of the calculations was to determine whether the theoretical results could provide any explanation for these observations and analyses of the $Al_2Cl_7^-$ structure.

The calculations were performed with use of the MNDO (Modified Neglect of Diatomic Overlap) method developed by Dewar et al.[12,13] To adequately model the species in the melts, it is necessary to account for the interactions of the chloroaluminate species with positive counterions in the melts. Inclusion

(8) Øye, H.A.; Rytter, E.; Klaeboe, P., Cyvin, S. *J.Acta Chem. Scand.* **1971**, *25*, 559.

(9) Klaeboe, P.; Rytter, E.; Sjørgren, C. E. *J. Mol. Struct.* **1984**, *113*, 213.

(10) Hvistendahl, J.; Klaeboe, P.; Rytter, E.; Øye, H. A. *Inorg. Chem.* **1984**, *23*, 706.

(11) Couch, T. W.; Lokken, D. A.; Corbett, J. D. *Inorg. Chem.* **1972**, *11*, 357.

(12) Dewar, M. J. S.; Thiel, W. *J. Am. Chem. Soc.* **1977**, *99*, 4899.

(13) Dewar, M. J. S.; Thiel, W. *J. Am. Chem. Soc.* **1977**, *99*, 4907.

of MEI⁺ ions in the calculation would be cumbersome indeed. Furthermore, the effect of substituting a smaller cation for MEI⁺ on the structures and energies of the anion species and their interactions are expected to be small as will be discussed later. Thus a recent modification to the MNDO program[14] which allows for the use of "sparkles" was employed. There are essentially point charges made to simulate positive ions of various size. An evaluation of the effectiveness of sparkles in improving the validity of the calculations was therefore an additional goal of this effort. Details of the MNDO method and the use of the sparkles are presented in the next section on Theoretical Methods.

Theoretical Methods

In order to obtain useful results in minimum computer time, the semiempirical method MNDO was used. MNDO is an all-valence-electron SCF method. In its current form, geometry optimizations and force calculations are routinely carried out. MNDO has been parametrized for all the elements in the chloroaluminate melt and is available through the Quantum Chemistry Program Exchange in the program MOPAC.[15] Because MNDO is well documented,[12] only those modifications to the standard formulation will be discussed here.

The chloroaluminate melt consists of highly ionized moieties. Our interest focuses on the geometry and energetics of the anions; the cation was of secondary interest, and its inclusion in the calculations, although necessary, was an inconvenience. The effect of including large melt cations would be to slow down the calculation considerably and use a large amount of computer memory.

The exact nature of the counterion does not significantly affect our results. Since only the electric field produced by it is needed, the cation counterion was modeled by using a point charge. The effect of this is to considerably reduce the time required for the calculations.

Sparkles. The chemical behavior of most strong alkali ions is very similar—they all behave like unipositive point charges and differ only in their size, a sodium ion being smaller than a potassium ion, which in turn is smaller than a tetramethylammonium ion. As most of the electron density in the valence shell has been removed on forming the ion, the exact nature of the valence orbitals is not important, and for our purposes, the valence orbitals on the counterions can be ignored, the effect of this being to produce an ion which has an exactly +1 charge. To indicate that the only chemical property the resulting entities have is purely electrostatic, they are called "sparkles". Although the valence electron density is unimportant, the core electrons do give rise to a core–core repulsion term. In MNDO this repulsion is represented by a term of form

$$E(\text{core–core}) = Z_1 Z_2 Y_{1,2} \exp(-\alpha r_{12})$$

where Z_1 and Z_2 are the core charges, $Y_{1,2}$ and α are adjustable parameters, and r_{12} is the internuclear distance.

The sparkles are differentiated by their α values; a large value for α corresponds to a small ion. Specific values of α for lithium (1.53 Å⁻¹), sodium (1.32 Å⁻¹), and potassium (1.16 Å⁻¹) were chosen because they were found to result in MNDO predictions of the interatomic distances in the chlorides of these alkali metals which agree with experimental values.

To date, sparkles have been used only for setting up an electric field gradient in order to calculate polarizability.[14] Other uses anticipated include the use of pairs of sparkles of opposite charge to mimic unpolarizable molecules with dipoles in polar solvent studies, for example. To facilitate this application, such isolated pairs of sparkles are defined as having zero energy.

In all calculations involving sparkles, they are treated in precisely the same manner as normal ions. For example, in a force calculation the vibrations due to sparkles moving can readily be calculated.

Currently the alkali metals are being parametrized, but until parameters are available, current releases of MOPAC will include the lithium, sodium, and potassium-like sparkles.

Techniques for Obtaining Transition States. The reaction being considered is relatively simple, involving only simple bond-making and bond-breaking. As a result, an internal coordinate in the complex could be identified with the reaction path coordinate. By optimizing the geometry at fixed values of this coordinate, the transition state was identified. Of course, this very simple technique for obtaining transition states is only applicable to systems for which no ambiguity exists regarding the main features of the reaction mechanism.

The standard test for characterizing a transition state—calculating the force constants and verifying that one and only one negative eigenvalue

(14) Dewar, M. J. S.; Stewart, J. J. P. *Chem. Phys. Lett.* **1984**, *111*, 416.

(15) Stewart, J. J. P. *QCPE* **1983**, No. 455.

SYSTEM AlCl$_4^-$ WITH	BOND LENGTHS, Å		ANGLES	
	a	b$_{ave}$	A	B
isolated	2.15	2.15	109.5°	109.5°
K$^+$	2.11	2.16	113.2°	105.5°
Na$^+$	2.10	2.16	114.1°	104.5°
Li$^+$	2.10	2.16	115.3°	103.0°
Te$_4^{2+}$*			107.0	
		2.09	107.1	
		2.11	108.2	
		2.13	109.2	
		2.15	111.2	
			113.8	

*Couch et al.[11]

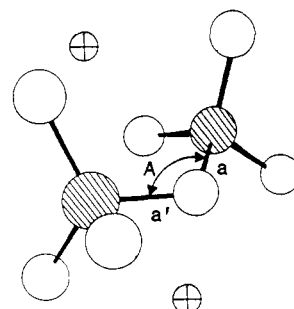**Figure 3.** MNDO structure for AlCl$_3$ and comparison with experimental results.

exists—was performed successfully on all candidate systems.

Results and Discussion

Molecular Geometries. Figure 3 shows the MNDO-calculated geometry of the AlCl$_4^-$ ion compared with X-ray spectrographic results from Couch et al.[11] The MNDO prediction for the isolated anion is a tetrahedral structure with Al–Cl distances of 2.15 Å. This compares quite favorably with the structure reported by Couch et al. for the AlCl$_4^-$ ion in the solid phase with a Te$_4^{2+}$ counterion. Addition of a single sparkle into the calculation produces a slight lengthening of the three Al–Cl bonds to the chlorines which associate with the sparkle, as well as a slight decrease in the Al–Cl bond length to the fourth, unassociated chlorine. The symmetry drops to C_{3v}, with the small Li$^+$ ion producing the largest distortion to the tetrahedral structure. If two sparkles are placed around the AlCl$_4^-$ anion, they align themselves on opposite sides of the anion, with a sparkle–aluminum–sparkle angle of 180°. Each sparkle associates with two chlorines resulting in D_{2d} symmetry.

The Al$_2$Cl$_7^-$ ion is a much more interesting species. Figure 4 shows the MNDO geometry, which is a bridged structure with one of the chlorines bonded to both aluminum atoms in a 2-electron, 3-center bond. It has an effective symmetry of C_{2v}, since rotations around the bridging Cl–Al axes are only slightly hindered (rotation barrier of about 0.4 kcal mol^{-1}). The isolated anion is predicted to have an Al–Cl–Al bridging angle of about 125°. Figure 4 also shows the solid–state salt results of Couch et al. for Al$_2$Cl$_7^-$. MNDO correctly predicts the bridging Cl–Al distance to be stretched by about 8% as compared with the terminal Cl–Al distances. The experimental bridging angle is somewhat less than the calculated angle.

Even though it is clear that the anion is a bent C_{2v} structure in the solid salt with a Te$_4^{2+}$ counterion, there is some controversy as to whether it is bent or linear in the molten salt. Hvistendahl et al.[10] claim that a linear structure, i.e., D_{3d} symmetry, for the Al$_2$Cl$_7^-$ in alkali chloride/AlCl$_3$ melts is consistent with the most direct interpretation of Raman and IR spectra observed at 473 K. They note that an exception is LiAl$_2$Cl$_7$ in which the lithium counterion appears to be small enough to stabilize Al$_2$Cl$_7^-$ in the bent structure forming into what they refer to as the "Li$^+$Al$_2$Cl$_7^-$ cage model". With this in mind, we varied the size and number of counterions around the Al$_2$Cl$_7^-$ ion in an attempt to induce a linear structure as shown in Figure 4. These variations produced small changes in the Al–Cl distances on the order of the ones

SYSTEM Al$_2$Cl$_7^-$ WITH	A	BOND LENGTH, Å		BRIDGE INVERSION BARRIER kcal mol^{-1}
		a	a'	
(Isolated)	124.9°	2.30	2.30	5.2
K$^+$	124.7°	2.29	2.29	5.9
Na$^+$	124.0°	2.29	2.29	6.4
Li$^+$	123.5°	2.27	2.37	6.3
2K$^+$	123.6°	2.30	2.30	5.5
2Na$^+$	123.4°	2.30	2.30	6.0
2Li$^+$	123.9°	2.30	2.30	7.4
2K$^+$ + 2AlCl$_4^-$	124.0°	2.28	2.31	
4K$^+$ + 2AlCl$_4^-$	124.3°	2.30	2.30	
3K$^+$ + 3AlCl$_4^-$	122.8°	2.29	2.31	
Te$_4^{2+}$(s)*	110.8°	2.22	2.26	
1Pd$_2$(C$_6$H$_6$)1^{2+}*	115.6°	2.29	2.34	

*Couch et al.[11]

Figure 4. MNDO structure for Al$_2$Cl$_7^-$ and comparison with experimental results.

previously observed for AlCl$_4^-$, but the bridging angle changed by no more than 2° from its isolated value of 125°. Even addition of several stacks of cation sparkles associated with AlCl$_4^-$ anions around the Al$_2$Cl$_7^-$ anion only slightly changed the bridging angle. Thus, within the limits of our ability to model ionic environments around an ion with MNDO using the sparkles, we conclude that the Al$_2$Cl$_7^-$ ion is a bent C_2 structure (or effectively C_{2v} if we view the end chlorines as freely rotating about the Cl–Al bond).

Another possible reason why the vibrational analysis may indicate a linear structure while our calculations predict a bent structure is a very low barrier to inversion at the bridging chlorine. This was also proposed by Hvistendahl et al.,[10] who suggested that molten MAl$_2$Cl$_7$ compounds other than LiAl$_2$Cl$_7$ might have a "limp Cl bridge with random fluctuations around the linear configuration". Thus we calculated the inversion barrier for the Al$_2$Cl$_7^-$ ion for a variety of sizes and numbers of associated sparkles (Figure 4). We found that the predicted inversion barrier varied only slightly, ranging from 5 to 8 kcal mol^{-1} for all of the environments. Compared with a thermal energy (RT) of about 0.9 kcal mol^{-1} at 473 K, these predicted barriers appear large enough to make it unlikely that a linear-averaged structure is the one observed.

Vibrational Analysis. In an effort to resolve the apparent discrepancy between the D_{3d} assignment based on the analysis of the spectra of Al$_2$Cl$_7^-$ and the C_2 assignment based on our MNDO results, we calculated vibrational frequencies of the Al$_2$Cl$_7^-$ ion in three different environments. The results of these calculations, along with available experimental data on the vibrational frequencies of this anion, are given in Table I. In Figure 5 we have also reproduced the IR emission spectrum of molten KAl$_2$Cl$_7$ at 200 °C obtained by Hvistendahl et al.[10] for comparison with the MNDO-predicted fundamentals for the Al$_2$Cl$_7^-$ in our most realistic modelling of the melt environment, i.e., the "stack model" described in the section below on the exchange reaction. The theoretical lines are shown with heights directly proportional to the squared total transition dipole moments calculated by MNDO for these fundamental vibrations.

A rather remarkable agreement between the MNDO frequencies and the experimental results can be seen if we divide the IR spectrum into four parts. We exclude from the analysis the bands above 600 cm^{-1} which are almost certainly combination bands.[10]

Table I. Vibrational Frequencies of Al$_2$Cl$_7^-$

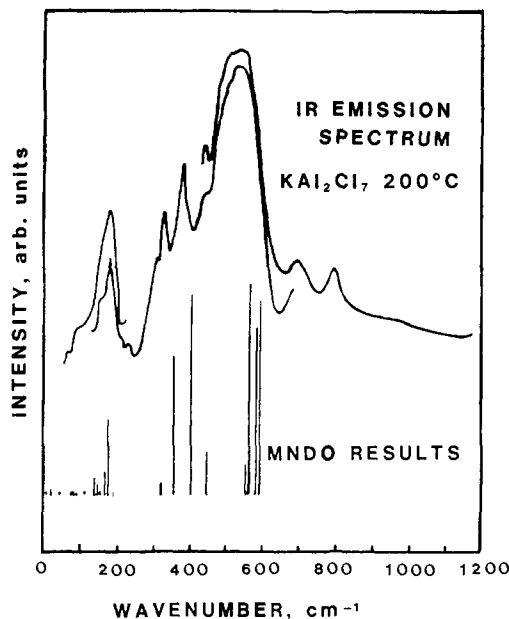| MNDO results				spectroscopic frequencies[10]		
fundamentals (cm^{-1})				IR (cm^{-1})	Raman (cm^{-1})	
isolated	with K$^+$ sparkle	stack model	assignment (C$_2$)			assignments (D$_{3d}$)
14	5	7	A			
11	30	21	B			
41	48	46	A			
77	74	79	B			
78	80	81	A	} Al–Cl$_3$ def and Al–Cl–Al bending		
87	89	88	A			
107	109	109	B	97	97	K$^+$---Al$_2$Cl$_7^-$
135	144	138	A			
144	147	145	B			
148	147	149	A			
162	161	164	B	158		ν_{12} E$_u$ } Al$_2$Cl$_3$ def
173	172	172	B	} Al–Cl$_3$ def	161	ν_3 A$_{1g}$
184	185	185	A	179		ν_7 A$_{2u}$
315	318	320	A	308	311	ν_2 A$_{1g}$ } Al–Cl–Al stretch
348	350	351	B	} Al–Cl–Al stretch	331	ν_6 A$_{2u}$
401	405	399	B	381		ν_5 A$_{2u}$ } AlCl$_3$ stretch
447	454	448	A	439	432	ν_1 A$_{1g}$
556	537	551	B			
560	548	556	A	} Al–Cl$_3$ stretch		
572	581	576	B	525		ν_{11} E$_u$ } AlCl$_3$ stretch
573	592	583	A			

Figure 5. Comparison of IR spectrum of KAl$_2$Cl$_7$ at 200 °C obtained by Hvistendahl et al.[10] with MNDO results.

(a) 158–179 cm^{-1}. In this region there are apparently three bands which correspond to deformations of the AlCl$_3$ end groups in the analysis which assigns the Al$_2$Cl$_7^-$ to the D_{3d} point group.[9] The symmetry species assigned were E$_u$, A$_{1g}$, and A$_{2u}$ which correlate with [A + B], A, and B, respectively, in the C_2 point group. The MNDO results show three fundamentals in this frequency range which also correspond to deformation of the AlCl$_3$ end groups and are assigned to B, B, and A symmetry species of the C_2 point group. We further note that MNDO predicts three other frequencies close to this group—at 138, 145, and 149 cm^{-1}—which have intensities that fit the experimental spectrum.

(b) 308–439 cm^{-1}. The D_{3d} analysis identifies these four bands as Al–Cl–Al (or bridge) stretching and end-AlCl$_3$ stretching. This is the same as the motions described by the MNDO results. Further the two A$_{2u}$ and two A$_{1g}$ assignments correlated to the two A and two B assignments based on the MNDO descriptions of the vibrations in the C_2 molecule. This agreement also extends to the relative intensities of the bands as is clearly seen in Figure 5.

(c) **Broad Band at 525 cm^{-1}.** This actually appears to be a group of bands corresponding to AlCl$_3$ stretching modes. The E$_u$ assignment in D_{3d} correlates with the (A + B) species assigned to the MNDO results. The frequencies calculated are fairly close together and similar in transition dipole moment, so they could be expected to overlap considerably. Moreover, since the vibrations are Al–Cl stretches on the exposed AlCl$_3$ ends of the ion, their observed bands should be highly susceptible to collisional broadening in the molten phase. That the MNDO frequencies are somewhat higher than the observed frequencies may be at least partly explained by the fact that the stack model does not have the Al$_2$Cl$_7^-$ "surrounded" by interacting ions so it is closer to a gas-phase than to a melt-like configuration. As a result, the force constants for the Al$_2$Cl$_7^-$ vibrations in the stack model will not be decreased by associations with surrounding ions to the same extent as must occur in the actual melt.

(d) **Bands at Frequencies Lower Than 158 cm^{-1}.** A comparison of the low-frequency MNDO results with the spectrum shown in Figure 5 suggests that all the remaining MNDO frequencies may be present in the lower frequency wing of the observed band peaking at 179 cm^{-1}. For the same reasons as in (c) above, we would not expect the spectrum of the melt to show these fundamentals as sharp, unbroadened bands.

These comparisons lead us to conclude that the IR emission spectrum obtained by Hvistendahl et al.[10] is consistent with a C_2 or C_{2v} (assuming free AlCl$_3$ rotation) structure for the Al$_2$Cl$_7^-$ ion. The close groupings of bands predicted by MNDO in the regions described in (a) and (b) above provides an explanation for the previous interpretations of the spectra in terms of a D_{3d} structure for Al$_2$Cl$_7^-$. It is easy to see how the observed spectrum can be viewed as showing only the seven IR active fundamentals expected for the D_{3d} structure rather than the 21 expected for a C_2 or C_{2v} structure. The other "missing" fundamentals are at low intensity and in a frequency range at or below the detection limits of the instrumentation available.

Exchange Reaction. We next report the results for the exchange reaction (eq 3) observed in ^{27}Al NMR spectra of N = 0.60 melts, as previously discussed. We modelled this exchange reaction in a variety of ionic environments. In each of the three cases described below, the reaction coordinate was chosen to be the distance between one of the chlorines on the Al*Cl$_4^-$ and one of the aluminums on the Al$_2$Cl$_7^-$. This reaction coordinate was varied between a distance large enough to reproduce the heats of formation of the isolated reactants and a distance small enough to produce the products. The geometries of all stationary points determined from this reaction path were fully optimized, and all
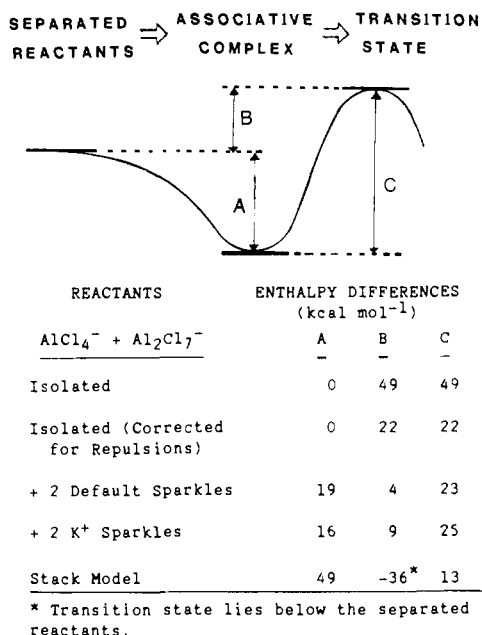
SEPARATED ⇒ ASSOCIATIVE ⇒ TRANSITION
REACTANTS 　　 COMPLEX 　　 STATE

REACTANTS	ENTHALPY DIFFERENCES (kcal mol^{-1})		
AlCl$_4^-$ + Al$_2$Cl$_7^-$	A	B	C
Isolated	0	49	49
Isolated (Corrected for Repulsions)	0	22	22
+ 2 Default Sparkles	19	4	23
+ 2 K$^+$ Sparkles	16	9	25
Stack Model	49	-36*	13

* Transition state lies below the separated reactants.

Figure 6. Reaction profiles for the ^{27}Al NMR exchange reaction, eq 3.

REACTANTS	BOND LENGTHS, Å	
AlCl$_4^-$ + Al$_2$Cl$_7^-$	a	a'
Isolated	2.96	2.98
With 2 Default Sparkles	2.70	2.92
With 2 K$^+$ Sparkles	2.71	2.82
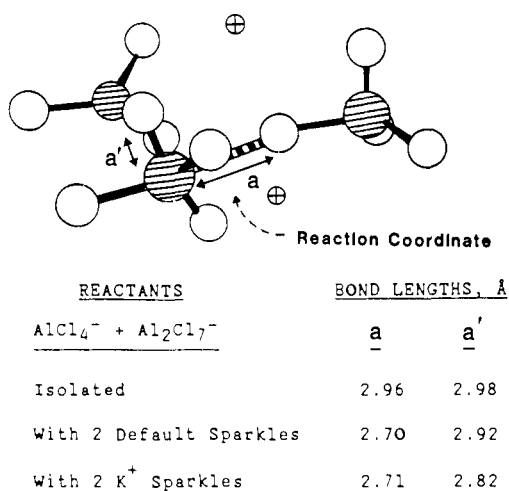
Figure 7. Transition state for the ^{27}Al NMR exchange reaction with fully optimized geometry.

suspected transition states were proven to be such by the presence of one, and only one, negative force constant. Figure 6 shows the relative heats of formation as the reaction coordinate is changed, and Figures 7 and 8 show the transition-state geometries.

(a) Isolated Ions. The first environment that we considered was that of the isolated anions, analogous to gas phase. Since both reactants are anions, we expected a substantial barrier due to Coulombic repulsions, and that was confirmed. The reaction proceeded as expected, with the AlCl$_4^-$ being split off from the Al$_2$Cl$_7^-$ as the new Al–Al bond formed. The barrier, however, was 49 kcal mol^{-1}, and both the Cl–Al distances in the bridge were almost 3.0 Å at the transition state. There were no other stationary points along the reaction path except for the transition-state value, with the relative heats of formation rising monotonically to the transition state and then falling monotonically to the product value. A crude way to correct for the overestimation of the Coulombic repulsions (with no ionic environment) is to subtract all of the Coulombic repulsions calculated for each pair of atoms (one in each reactant) based on the MNDO-calculated atomic charges. When this was done at the transition-state geometry, the barrier was lowered to 22 kcal mol^{-1}. This same correction was made to various points along the reaction path to ensure that no new stationary points were introduced.

(b) Ions and Two Sparkles. Introduction of two counterions into the calculation resulted in the occurrence of a mimimum along
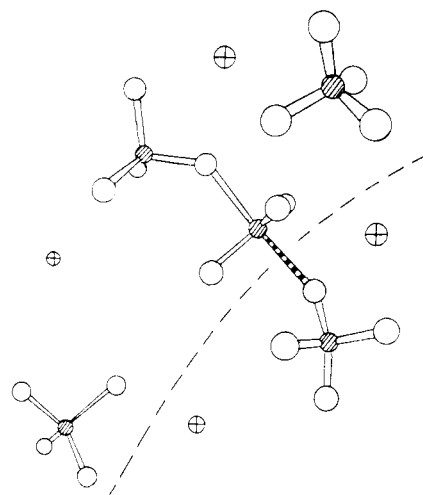

Figure 8. Transition state for the ^{27}Al NMR exchange reaction with fully optimized geometry with the "stack model". The dashed line separates the two stacks associated with the reacting anions.

the reaction path (which we call the associative complex) resulting from mutual attraction of the counterions by both anions, as shown in Figure 6. This mimimum energy point in the cases with two sparkles added to the system occurred at a distance of about 7 Å. The net stabilization is approximately 20 kcal mol^{-1} compared with the isolated reactants (AlCl$_4^-$ and Al$_2$Cl$_7^-$ each associated with a single sparkle). The transition state lies 4 kcal mol^{-1} above the isolated reactants in the case of the default-size sparkles, and 9 kcal mol^{-1} in the case of the K$^+$ sparkles. In both cases, the transition state is about 25 kcal mol^{-1} above the associative complex. Figure 7 shows that the Cl–Al reaction coordinate distance is now about 2.7 Å at the transition state as compared with the 3.0 Å observed when no sparkles were used.

(c) Stack Model. Our most realistic effort to model the reaction occurring in the melt involved placing the Al$_2$Cl$_7^-$ ion in a "stack" by locating it between two ion pairs, each composed of a potassium-size sparkle and an associated AlCl$_4^-$ ion. The incoming AlCl$_4^-$ ion has two potassium-size sparkles constrained to opposite sides of it in order to give it a "stack-like" environment as well and to make the overall system electrically neutral. In our initial reaction path calculation, we also constrained the K$^+$–Al$_2$Cl$_7^-$–K$^+$ angle to 180° but allowed the AlCl$_4^-$ ions associated with the K$^+$ ions to change their orientation. After locating the associative complex and transition state, we recalculated them allowing all geometrical constraints to relax, and the final totally optimized results differed by less than 1 kcal mol^{-1} from the constrained results. In addition, complete optimization changed the geometries very little from the constrained geometries, further supporting the stack model. The final results for the reaction stack model shown in Figures 6 and 8 are for fully optimized stationary points. The minimum along the reaction path occurred at about 10 Å, and this associative complex is stabilized by 49 kcal mol^{-1} compared with the isolated reactant groups. The transition state occurred at a Cl–Al distance of 2.7 Å, and its heat of formation was 13 kcal mol^{-1} above the associative complex. Note that the transition state heat of formation is actually 36 kcal mol^{-1} *less* than that of the isolated reactants.

(d) Activation Energy. It is not immediately obvious how to interpret these results in terms of a predicted activation energy for the reaction. In the gas phase, of course, the predicted activation energy would simply be the difference in the heat of formation of the transition state and the sum of the heats of formation of the isolated reactants, corrected by RT to account for the difference between activation energy and activation enthalpy. In our modelling of the ionic environment in the molten salt, we must consider not only the isolated reactants but also the presence of the stable associative complex along the reaction path. If we were to model the melt in its entirety, the starting point for the reaction would be the equilibrium structure of the melt. In

this work, the stable associative complex is the closest we approach the equilibrium condition. Thus, if we interpret the difference in heats of formation between the transition state and the associative complex to be the activation energy for the reaction as it would proceed in the melt, any error that we obtain would be due primarily to our incomplete modelling of the melt structure. A better, more complete modelling of the melt structure, involving introduction of more ions around the reacting species into the calculation, should yield a more accurate answer. We do note that our best modelling of the melt in this work, the stack model, produced a predicted activation energy of 13 kcal mol^{-1}, very close to the apparent experimental value. It is also significant that each step we took to more realistically model the environment of the reactants decreased the difference between the experimental and calculated energy activation.

Conclusions

The $Al_2Cl_7^-$ anion is predicted to be a bent, effectively C_{2v} structure. This prediction is invariant to a variety of ionic environments around the anion. In addition, the barrier to inversion at the bridging chlorine is too high to conclude that a linear-averaged structure could have been observed in vibrational spectra of this anion. Our calculated vibrational frequencies and transition dipole moments for the anion agree well with available experimental data. Previous interpretations of the observed vibrational spectra indicating D_{3d} symmetry can be understood in light of the fact that many of the vibrational frequencies are too close together and broadened by interactions with the alkali couterions to be readily observed as separate bands. The excellent agreement between the observed IR spectrum and the MNDO calculated spectrum (including the predicted intensities) confirms that the MNDO method can be very useful in interpretation of IR spectra of similar systems.

The use of sparkles in MNDO seems to be an effective way of modelling ionic interactions in molten salts. They are effective in shielding reacting species of the same charge from each other until they get close enough to react, as one would expect in the true melt. Modelling the structure of the melt with a combination of the sparkles for positive charges and additional $AlCl_4^-$ anions appears to be a promising way to study melt structure and reactions which take place in the melt.

On the basis of our admittedly incomplete model of the melt, the exchange reaction between $AlCl_4^-$ and $Al_2Cl_7^-$ is probably the reaction which causes the ^{27}Al NMR line shape behavior in the MEICl/$AlCl_3$ system. The predicted activation energy for this reaction is very close to the experimental value.

We are continuing calculations on improved models of the melt. We are adding a larger number of ions in the ionic environment of the reacting species. In addition, we will also attempt to actually use the imidazolium cation itself in the calculation as the counterion. Either or both of these improvements should allow us to obtain even better estimates of melt structures and the energetics of reactions taking place in the melts.

An ab Initio Molecular Orbital Study on Rearrangement/Fragmentation Processes of Isomeric CH₃N⁺· Ions

Einar Uggerud*[†] and Helmut Schwarz*[‡]

Contribution from the Department of Chemistry, University of Oslo, N-0315 Oslo 3, Norway, and the Institut für Organische Chemie der Technischen Universität Berlin, D-1000 Berlin 12, Federal Republic of Germany. Received February 19, 1985

Abstract: The potential energy surface of the $CH_3N^+·$ system has been investigated using ab initio molecular orbital theory. In accordance with experiment it is found that the two isomers, methylenimine radical cation, $CH_2NH^+·$ (1), and aminomethylene cation, $CHNH_2^+·$ (2), are found to be separated by a high-energy barrier (239 kJ mol^{-1}) which largely prevents them from isomerizing prior to microsecond fragmentation. However, contrary to previous interpretations, it is argued that the isomer CNH_2^+ is not formed in the course of H· loss from $CH_3N^+·$ under mass spectrometric conditions.

Introduction

During the last few years, the structure/reactivity problem of gaseous radical cations has received renewed attention. It has been demonstrated that in addition to the molecular ion, other ionic isomers exist for which the neutral counterparts are unknown. These structurally intriguing isomers are often found to have comparable if not lower heats of formation. Particular cases concern the so-called *distonic* ions,[1a] species which contain both

hyper- and hypovalent structure, and which do not obey the classical valence rules.[1]

A case in point concerns $CH_3N^+·$ isomers, which have been thoroughly investigated experimentally by Burgers et al.[2] By means of collisional activation (CA) mass spectrometry, isotopic labeling, and thermochemical measurements, Burgers et al.

[†] University of Oslo.
[‡] Technische Universität Berlin.

(1) (a) Yates, B. F.; Bouma, W. J.; Radom, L. *J. Am. Chem. Soc.* **1984**, *106*, 5805. (b) For a recent review and leading references, see: Schwarz, H. *Mass Spectrosc. (Tokyo)* **1984**, *32*, 3.
(2) Burgers, P. C.; Holmes, J. L.; Terlouw, J. K. *J. Am. Chem. Soc.* **1984**, *106*, 2762.